A Cyclic Damaged Plasticity Model: Implementation and Applications

Yuli Huang
Graduate Student Research Associate
Stephen A. Mahin
Byron and Elvira Nishkian Professor of Structural Engineering

Department of Civil and Environmental Engineering
University of California at Berkeley
Berkeley, CA 94720

Abstract

In analysis and design of structures subjected to earthquakes, the cyclic and dynamic nature of the response leads to complications. Material models need to account for cyclic plasticity, including deterioration and eventual failure due to low-cycle fatigue. A cyclic damage plasticity model MAT_DAMAGE_3 (MAT_153, LSTC 2007) is implemented to combine Armstrong-Frederick/Chaboche nonlinear kinematic hardening, isotropic hardening, and Lemaitre isotropic damage evolution based on continuum damage mechanics. By appropriately choosing parameters, this model can reproduce an approximation to the widely-accepted Manson-Coffin low-cycle fatigue rule without of cycle counting. This makes it possible to model the decrease in the material's ability to deform inelastically. The material model is applied to assess the behavior of a steel structure subjected to deterioration and failure.

Introduction

In seismic-resistant design, structural engineers are increasingly interested in prediction of inelastic response using nonlinear dynamic analysis procedures. It has been common to assume ideal ductile behavior for structural members. However, infinitely ductile models may not be adequate for seismic or other abnormal loading conditions, as inelastic demands will likely lead to deterioration and possible failure of members. These weakened members will in turn influence dynamic response and overall system stability. For structures subjected to earthquakes, the cyclic and dynamic nature of their response leads to further complications in that material models need to account for cyclic plasticity, including deterioration and eventual failure due to low-cycle fatigue.

The effects of sudden onset, quasi-brittle fracture are not considered in this work. It is assumed that a separate fracture-mechanics-based analysis would be carried out on individual fracture critical regions. The research presented herein includes situations where members rupture due to materials reaching and exceeding their ability to develop further inelastic deformations, either under monotonic or cyclic loading.

Steel braced frame structures provide the focus of this investigation. Experimental data for a Special Concentric Braced Frame (SCBF) subassembly subjected to cyclic lateral loading are summarized, followed by a review and evaluation of material models commonly used for structural steel. A cyclic damaged plasticity material model is then formulated and implemented. Finally, the new material model is used to compute the behavior of braced frame subassembly.

Special Concentric Braced Frame Experiment

The two story special concentric brace frame tested by Uriz and Mahin (2005) is shown in Figure 1. The frame suffered extensive damage to the braces in the lower level, to the columns at the base of the building and in the beam-to-column connections at the first floor level. A variety of behavior was observed, from yielding, local buckling, local tearing, brace fracture, column local buckling, and connection fracture (as reported in Uriz and Mahin, 2005). This specimen provides a good test of the ability of a computational model to predict behavior associated with members undergoing bending and axial load, lateral buckling, and local buckling, and rupture.

In the experiment, global lateral buckles formed in the lower level braces, with local buckling occurring near the brace midspans (Figure 1b). This resulted in a weak lower-story response, with nearly all inelastic behavior and damage concentrated in the lower level. This led to the complete rupture of the braces during the first excursion to the design level (Figure 1c), with failure of the lower level beam to column connections occurring soon thereafter (Figure 1d).

a) Test setup for SCBF

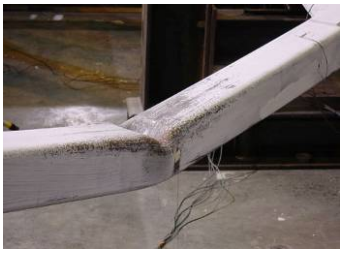

b) Buckling of brace

c) Fracture of brace

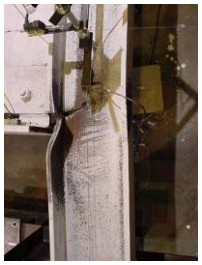

d) Fracture of connection

Figure 1: SCBF experiment results (Uriz and Mahin, 2005)

Review of Material Modeling For Structural Steel

For structural steel subjected to a severe loading history, such as a strong earthquake, it is recognized that several stages of behavior commonly exist during the course of member deterioration. Initially, it is assumed there are no macroscopic cracks, thus no stress or strain singularities associated with the material. The material is then loaded non-proportionally and cyclically under stress and strain histories of varying amplitude. Deterioration develops due to material and geometrical nonlinearities. Large plastic deformation and energy dissipation results in progressive failure of the material. Eventually, macroscopic cracks may initiate and extend up to size of the member.

Damage resulting from plastic deformation in ductile metals is mainly due to the formation of microvoids, which initiate either as a result of fracturing or debonding of inclusions, such as carbides and sulfides, from the ductile matrix. The growth and coalescence of microvoids under increasing plastic strain progressively reduces the material's ability to carry loads, and can result in complete failure. A proper modeling of this micro-void nucleation and growth mechanism is needed for the prediction of ductile failure in steel members and structures. In the context of continuum mechanics, coupled plasticity and damage models may be needed.

Modeling of plasticity
Isotropic hardening and/or kinematic hardening are commonly used to describe the plastic behavior of metal-like materials under complex loading conditions. Prager (1956) and Ziegler (1959) initiated the fundamental framework used for kinematic hardening rules. Armstrong and Frederick (1966) developed a nonlinear kinematic hardening rule that generalized its linear predecessor. In this model, the kinematic hardening component is defined to be an additive combination of a purely kinematic term (linear Prager/Ziegler hardening law) and a dynamic recovery term, which introduces the nonlinearity (fading memory effect of the strain path). The Armstrong and Frederick rule was further extended by Chaboche (1986, 1989), where an additive decomposition of the back stress was postulated. The evolution equation of each back stress component is of the Armstrong-Frederick type. The advantages of this superposition are a larger strain range can be realistically modeled, and a more accurate description of ratcheting is provided. These features allow modeling of inelastic deformation in metals that are subjected to cycles of load, resulting in significant inelastic deformation and, possibly, low-cycle fatigue failure. Discussion of these plasticity models can be found in Lemaitre and Chaboche (1990).

Models of damage and fracture under monotonic loading
Two alternative approaches are generally considered for material failure modeling: local approaches and global approaches. The local approach to fracture can be defined very generally as the combination of (1) the computation of local stress and deformation values in the most loaded zones of a component or structure, and (2) predefined models corresponding to various fracture mechanisms, such as cleavages, ductile fracture, fatigue, creep, stress-corrosion etc. (Rousselier, 1987). Many models have been developed since the initial studies of McClintock (1968) and Rice and Tracey (1969). Most local models can be written in the form of stress-modified critical plastic strain:

$$\text{Damage evolution} \quad D = \int F(\boldsymbol{\sigma}) G\left(\dot{\boldsymbol{\varepsilon}}^{pl}\right)$$

$$\text{Failure criterion} \quad D = D_c$$

where F is the stress modification function, G is the plastic strain function, D represents the damage in the material, and D_c is the critical damage at failure. For example, the model of Rice and Tracey (1969) can be written as

$$F(\boldsymbol{\sigma}) = \exp(1.5\, p/\bar{\sigma}) \quad G\left(\dot{\boldsymbol{\varepsilon}}^{pl}\right) = \dot{\bar{\varepsilon}}^{pl} = \sqrt{\frac{2}{3}\dot{\boldsymbol{\varepsilon}}^{pl} : \dot{\boldsymbol{\varepsilon}}^{pl}}$$

where p is hydrostatic stress, $\bar{\sigma}$ is von Mises stress and $\dot{\bar{\varepsilon}}^{pl}$ is equivalent plastic strain rate. For porous metal plasticity, i.e. the GTN model developed by Gurson, Tvergaard and Needleman

(Gurson 1977; Tvergaard and Needleman, 1984), together with the sophisticated yield function they developed, the void growth part is given by

$$F(\boldsymbol{\sigma})=1 \quad G\left(\dot{\boldsymbol{\varepsilon}}^{pl}\right)=\dot{\varepsilon}_v^{pl}=\dot{\boldsymbol{\varepsilon}}^{pl}:\boldsymbol{1}$$

where $\dot{\varepsilon}_v^{pl}$ is the volumetric plastic strain rate.

For the ductile damage model proposed by Lemaitre (Lemaitre, 1992; Dufailly and Lemaitre, 1995), which is based on continuum damage mechanisms (CDM) introduced by Kachanov (1958), the damage evolution function becomes

$$F(\boldsymbol{\sigma})=\left[\frac{Y}{S}\right]^{\mathrm{t}} \quad G\left(\dot{\boldsymbol{\varepsilon}}^{pl}\right)=\dot{\bar{\varepsilon}}^{pl}$$

where S is a material constant with energy density units, t is a dimensionless material constant, and Y is the internal energy density release rate, calculated as

$$Y=\frac{1}{2}\boldsymbol{\varepsilon}^{el}:\boldsymbol{D}^{el}:\boldsymbol{\varepsilon}^{el}$$

where $\boldsymbol{D}^{el}$ is fourth order elasticity tensor and $\boldsymbol{\varepsilon}^{el}$ is second order elastic strain tensor.

Predictions using the Rice and Tracey (1969) and the Lemaitre (1992) models have been previously compared. The equivalent plastic strain at fracture versus stress triaxiality have very similar trend. In the case of proportional loading (Rousselier, 1987) and non-proportional loading (Marini et al., 1985), the two models give similar results. Recently, Steglich et al. (2005) investigated the relationship between the CDM and the GTN models.

In contrast to local approaches, global approaches are based on asymptotic continuum mechanics analyses. Under some situations, single- or dual-parameter models can uniquely characterize crack tip condition. Well-known single-parameters are stress intensity K, J-integral, and CTOD (crack tip opening displacement), and a well-known dual-parameter formulation is based on the introduction of the T-stress that characterizes the crack tip constraint. All these parameters are defined at the global level of the crack medium, in the framework of fracture mechanics. They are applicable to a number of situations in which it is not necessary to know the exact state of stress, or of damage, in the vicinity of the crack tip. On the other hand, this approach may prove to be deficient, either because of the size of the cracks, because of a pronounced overall plasticity during ductile fracture, or because of loading history effects. A systematic comparative study of local and global models was reported by Xia and Shih (1995) using a representative volume element (RVE) method. It was shown that the size of elements representing the crack in local approaches is the key parameter linking local and global approaches.

Local models of damage and fracture under cyclic loading

Local approaches to modeling damage and fracture under cyclic loading are examined in this section. They are compared to the Manson-Coffin rule for low cycle fatigue. The Manson-

Coffin rule is a popular model for low-cycle fatigue due to its simplicity. Generally, it is written in the form

$$\frac{\Delta\varepsilon_p}{2} = \varepsilon'_f \left(2N_f\right)^c \tag{1}$$

where $\Delta\varepsilon_p/2$ is the amplitude of plastic strain, N_f is the number of cycles, ε'_f is the ductility coefficient and c is the ductility exponent. In 1953, Manson recognized the form of Equation (1) relating fatigue life and plastic strain, and suggested that the magnitude of $1/c$ was "in the neighborhood of three" (Manson, 1953). Coffin showed that for practical purposes the fatigue property c is approximately equal to -1/2 (Coffin, 1954) and that ε'_f is related to the monotonic fracture ductility ε_f (Tvernelli and Coffin 1959). In fact, c commonly ranges from -0.5 to -0.7 for most metals, with -0.6 as a representative value.

Despite a large amount of work to generalize this law to multiaxial states of stress (Morrow, 1964) and to complex histories of loading (Manson et al., 1971), it remains a model generally limited in its application to uniaxial periodic loading. Still, a wide variety of structure tests, component and material specimens have demonstrated the general validity of the Manson-Coffin relation, and the range for the coefficient c cited above.

Not much attention has been given to the possibility of incorporating damage into cyclic plasticity by means of micromechanics. Recent works on porous metal plasticity are those of Leblond et al. (1995), Besson and Guillemer-Neel (2003) and Cedergren et al. (2004). They introduced nonlinear kinematic hardening into the GTN model. As far as continuum damage mechanics is concerned, Pirondi and Bonora (2003) introduced unilateral conditions to model stiffness recover in tension-compression cyclic loading. Kanvinde and Deierlein (2004) extended the Rice and Tracey (1969) model to incorporate a cyclic void growth model.

Lemaitre (1992) has a relatively simple modification for damage evolution in cyclic loading

$$\dot{D} = \begin{cases} \left[\frac{Y}{S}\right]^t \dot{\bar{\varepsilon}}^{pl} & \sigma_1 > 0 \\ 0 & \text{otherwise} \end{cases}$$

where σ_1 is the maximum principal stress. So damage does not accumulate when all principle stresses are compressive. This damage evaluation rule is used in material MAT_DAMAGE_1 (MAT_104, LSTC 2007). In material MAT_DAMAGE_3 (MAT_153, LSTC 2007), it is revised for simpler implementation as:

$$\dot{D} = \begin{cases} \left[\frac{Y}{S}\right]^t \dot{\bar{\varepsilon}}^{pl} & \frac{p}{\bar{\sigma}} > -\frac{1}{3} \\ 0 & \text{otherwise} \end{cases} \tag{2}$$

It can be shown that this simplification has negligible effect for most states of stress.

It is worth mentioning that although the critical equivalent-plastic-strain approach ($F(\boldsymbol{\sigma})=1$, $G(\dot{\boldsymbol{\varepsilon}}^{pl})=\dot{\bar{\varepsilon}}^{pl}$) can be used in proportional loading, it is unsuitable for cyclic loading. As illustrated in Table 1 (and approximately in Figure 2), fatigue life (number of cycles to failure) will tend to be underestimated if large strain amplitude data is used to calibrate the parameters (by a factor of 4 in the table). Conversely the fatigue life will tend to be overestimated if small strain amplitude data is used to calibrate the parameters. This is one inherent, and important, drawback of applying the critical equivalent-plastic-strain criterion to cyclic loading. The other drawback is the triaxiality-independence of critical equivalent-plastic-strain criterion; the effect of triaxial constraint on the initiation of rupture is a well known phenomenon.

Depending upon cycle counting schemes, the rule only increments the damage state at the end of each cycle. This is not suitable for a fatigue life of a few cycles; it does not allow material point fracture until the end of a full cycle. Continuous damage models can resolve this difficulty by accumulating damage continuously. Because the basic trends predicted by the Manson-Coffin rule have been verified for most low-cycle fatigue data, it is meaningful to use the Manson-Coffin rule as a reference and to compare results predicted by specific continuous damage models to those from the Manson-Coffin rule.

As a comparison, the simplified continuum damage mechanics model in Equation (2) is evaluated for low-cycle fatigue and compared with the Manson-Coffin rule. A uniaxial-stress single-element model is subjected to a series of constant amplitude strain cycles with several amplitudes of maximum strain. These cyclic deformation histories are imposed until rupture of the material occurs. In this way, standard Manson-Coffin type plots can be prepared for the analysis results and these can be compared directly with the ideal experiment Manson-Coffin criteria. The results are shown in Figure 2. Predicted results agree with those computed with the Manson-Coffin rule, with the ductility exponent *c* ranging from -0.5 to -0.7; i.e., corresponding to typical values for metals. The simplified CDM model in Equation (2) is chosen as the damage evolution model for MAT_DAMAGE_3 (MAT_153, LSTC 2007). It is believed that some underlying relationship should be satisfied when continuum damage models match the Manson-Coffin relation. This suggests deeper investigation is needed.

It should be noted again that the low cycle fatigue criterion based on critical equivalent-plastic-strain results in a fixed ductility exponent *c* equal to -1. As such, it is not able to predict the correct trend of low-cycle fatigue for metals. Thus, while the effective-plastic-strain criterion can be calibrated for a particular material and specimen configuration subjected to a specific loading protocol, the same failure criterion might not be expected to work at other locations within the same structure, or for different loading histories.

Table 1: Simple illustration of the difference between predictions of number of cycles to failure for an ideal experiment following the Manson-Coffin relation

Test or prediction	Calibrated to large strain amplitude data			Calibrated to small strain amplitude data		
	Strain amplitude	Number of cycle to failure	Test/EPS	Strain amplitude	Number of cycle to failure	Test/EPS
Experiment	0.20	2	1.00	0.20	2	0.25
EPS* prediction	0.20	2		0.20	8	
Experiment	0.05	32	4.00	0.05	32	1.00
EPS predication	0.05	8		0.05	32	

* EPS - critical equivalent plastic strain criterion

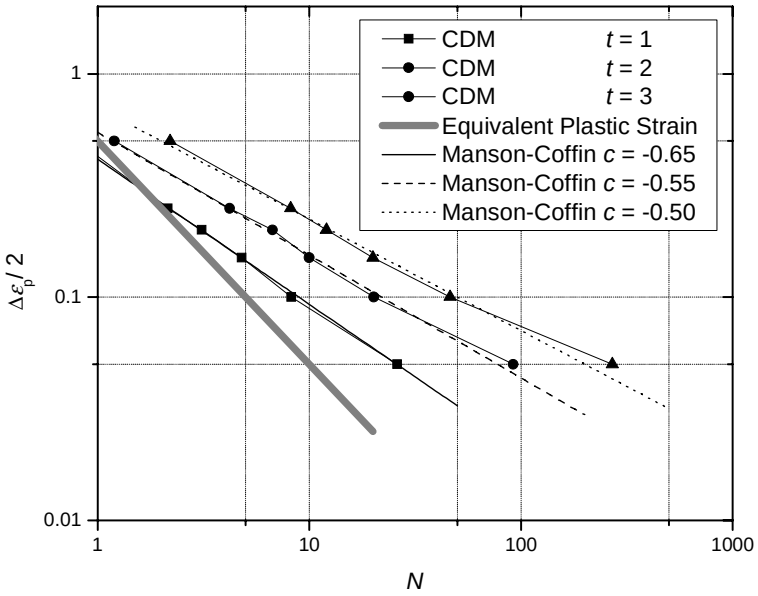

Figure 2: Fatigue relationships for CDM model (Eq. 2)

Formulation of A Cyclic Damaged Plasticity Material Model

The multi-component combined isotropic/kinematic plasticity and the damage evolution model based on continuum damage mechanics are used to formulate MAT_DAMAGE_3 (MAT_153)

The total strain rate $\dot{\boldsymbol{\varepsilon}}$ is written in terms of the elastic and plastic strain rates as

$$\dot{\boldsymbol{\varepsilon}} = \dot{\boldsymbol{\varepsilon}}^{el} + \dot{\boldsymbol{\varepsilon}}^{pl}$$

The elastic behavior is modeled as linear isotropic elastic

$$\boldsymbol{\sigma} = \boldsymbol{D}^{el} : \boldsymbol{\varepsilon}^{el}$$

where $\boldsymbol{D}^{el}$ represents the fourth-order elasticity tensor

$$\boldsymbol{D}^{el} = \kappa \boldsymbol{1} \otimes \boldsymbol{1} + 2\mu \left(\boldsymbol{I} - \frac{1}{3} \boldsymbol{1} \otimes \boldsymbol{1} \right)$$

and $\boldsymbol{\sigma}$ and $\boldsymbol{\varepsilon}^{el}$ are the second-order stress and elastic strain tensors, respectively.

The plasticity model is pressure-independent. The yield surface is defined by the function

$$F = \bar{\sigma} - \sigma_y = 0$$

where σ_y is uniaxial yield stress, and $\bar{\sigma}$ is the equivalent Mises stress, with respect to the deviatoric effective stress

$$\boldsymbol{s}_e = \mathrm{dev}[\boldsymbol{\sigma}] - \boldsymbol{\alpha} = \boldsymbol{s} - \boldsymbol{\alpha}$$

where $\boldsymbol{s}$ is deviatoric stress and $\boldsymbol{\alpha}$ is the back stress, which is decomposed into several components

$$\boldsymbol{\alpha} = \sum_j \boldsymbol{\alpha}_j$$

The equivalent Mises stress is defined as

$$\bar{\sigma}(\boldsymbol{s}_e) = \sqrt{\frac{3}{2}\boldsymbol{s}_e : \boldsymbol{s}_e} = \sqrt{\frac{3}{2}}\|\boldsymbol{s}_e\|$$

The model assumes associated plastic flow

$$\dot{\boldsymbol{\varepsilon}}^{pl} = \frac{\partial F}{\partial \boldsymbol{\sigma}}\mathrm{d}\lambda = \frac{3}{2}\frac{\boldsymbol{s}_e}{\bar{\sigma}}\mathrm{d}\lambda = \frac{3}{2}\boldsymbol{n}\mathrm{d}\lambda$$

where $\mathrm{d}\lambda$ is the plastic consistency parameter, and $\boldsymbol{n}$ is the flow direction

$$\boldsymbol{n} = \frac{\boldsymbol{s}_e}{\bar{\sigma}}$$

which is *not* a unit vector and its norm

$$\|\boldsymbol{n}\| = \sqrt{\frac{2}{3}}$$

For the von Mises criterion, $\mathrm{d}\lambda = \dot{\bar{\varepsilon}}^{pl}$, and $\dot{\bar{\varepsilon}}^{pl}$ is the equivalent plastic strain rate

$$\dot{\bar{\varepsilon}}^{pl} = \sqrt{\frac{2}{3}\dot{\boldsymbol{\varepsilon}}^{pl} : \dot{\boldsymbol{\varepsilon}}^{pl}}$$

where $\dot{\bar{\varepsilon}}^{pl}$ represents the rate of plastic flow.

The size of the yield surface σ_y is a user-defined function of equivalent plastic strain $\bar{\varepsilon}^{pl}$, for materials that either cyclically harden or soften.

$$\sigma_y = \sigma_y\left(\bar{\varepsilon}^{pl}\right)$$

The evolution of the kinematic component of the model is defined as

$$\dot{\alpha}_j = \frac{2}{3} C_j \dot{\varepsilon}^{pl} - \gamma_j \alpha_j \dot{\bar{\varepsilon}}^{pl} = \left[C_j \mathbf{n} - \gamma_j \alpha_j \right] \dot{\bar{\varepsilon}}^{pl} \tag{3}$$

where C_j and γ_j are material parameters. The recall term $\gamma_j \alpha_j \dot{\bar{\varepsilon}}^{pl}$ introduces the nonlinearity in the evolution law. The law can be degenerated into linear kinematic by setting only one α component and taking $\gamma = 0$. Note that a two-component kinematic hardening model equivalent to Equation (3) is adopted in material MAT_ANISOTROPIC_VISCOPLASTIC (MAT_103, LSTC 2007).

Finally, the damage variable increment is updated as

$$\Delta D = \begin{cases} \left[\frac{Y}{S} \right]^t \Delta \bar{\varepsilon}^{pl} & \bar{\varepsilon}^{pl} > \bar{\varepsilon}_d^{pl} \text{ and } \frac{p}{\bar{\sigma}} > -\frac{1}{3} \\ 0 & \text{otherwise} \end{cases}$$

where $p/\bar{\sigma}$ is the stress triaxiality, $\bar{\varepsilon}_d^{pl}$ is damage threshold, *S* is material constant with units of energy density, and *Y* is internal energy density release rate.

Application of Damaged Plasticity Model

Finite element analyses were conducted to assess the ability of the damaged plasticity model to simulate the hysteretic behavior of steel braced frame assemblages under cyclic loading. The focus is on prediction of local buckling and the evolution of damage due to low-cycle fatigue.

A finite element model was developed for the braced frame subassembly described previously, using shell elements. The choice of shell elements instead of solid or beam elements is simply to reduce the number of degrees of freedom and computational time. For a steel structure, solid elements are more computationally expensive as more solid elements are required through the thickness of the brace tube to capture the combined membrane and plate actions. Beam elements assume plane sections remain plane during deformation and the sectional coordinates of each integration point remain constant during the course of an analysis. This makes it impossible to model local buckling of a tube-section brace using beam elements.

Crack initiation and propagation is modeled by element erosion (removal of shell elements). Mesh convergence is examined below using progressively refined FE meshes. Both equivalent plastic strain and the damage variable are convergent when the element size is at the scale of the shell thickness. After crack initiation, the gradients of both equivalent plastic strain and the damage variable are much higher. Mesh sizes larger than the material characteristic length will result in a larger energy release rate at the crack tip (Xia and Shih, 1995). In addition, larger element sizes will blunt the crack front to an unrealistic size. However, it turns out that before the crack tip behaves inelastically, the strength and stiffness of the brace member have significantly deteriorated due to lateral and local buckling. Therefore, although there is an overly ductile

behavior locally, the crack front blunting due to use of large element sizes has less influence on overall behavior of the structure. A choice of shell element size at about the shell thickness achieves an overall model that is simple with reasonable accuracy.

In the model of the braced frame subassembly, the top-level displacement is prescribed as the boundary condition. The base is fixed and some out-of-plane constraint is applied at points around column ends and beam midspans, as they were in the experiment. The analysis results are shown in Figures 3 and 4. Crack initiation and propagation is captured (Figure 3a and 3b); buckling and fracture of brace is accurately modeled (Figure 3c). In addition, the simulated damage and fracture at the beam-column connection matches the experiment (Figure 3d). These simulations show that the cyclic damaged plasticity model is reasonable and useful for damage evaluation in steel structures. Figure 4 shows the base shear-roof displacement hysteresis curves for the experiment and numerical analysis, respectively. It is observed that strength, stiffness and deterioration in overall behavior of the braced frame is well simulated.

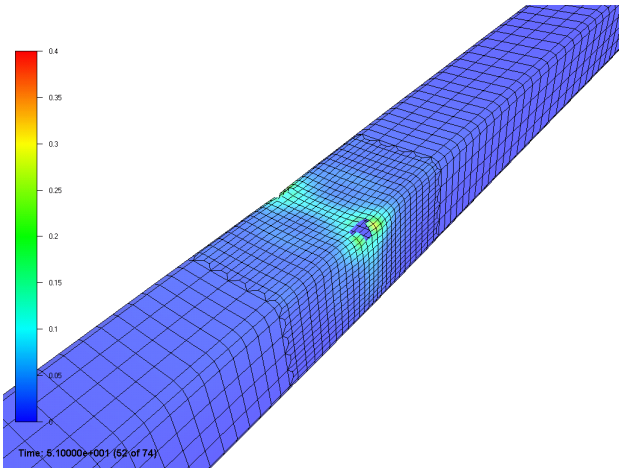

a) Crack initiation

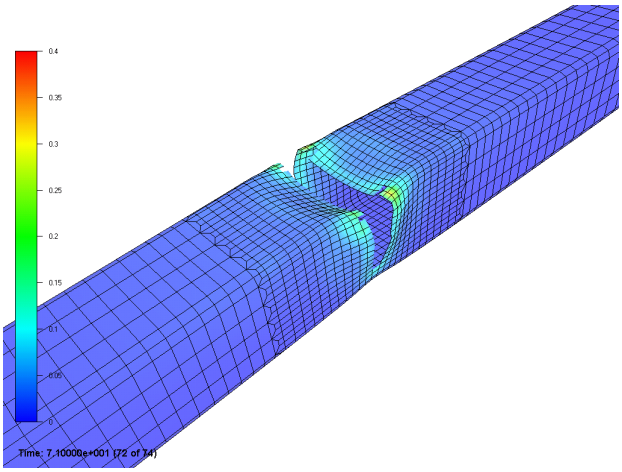

b) Crack propagation

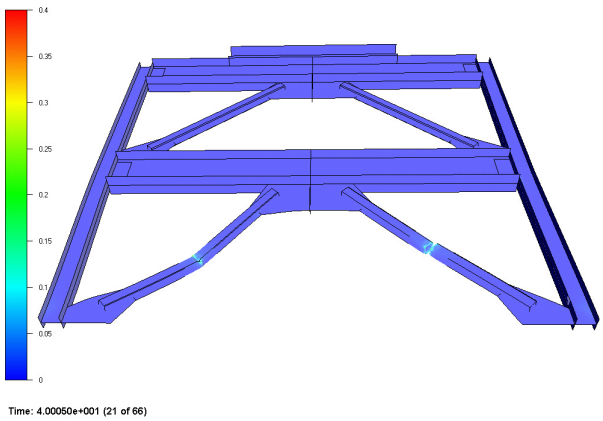

c) Damage and fracture of brace

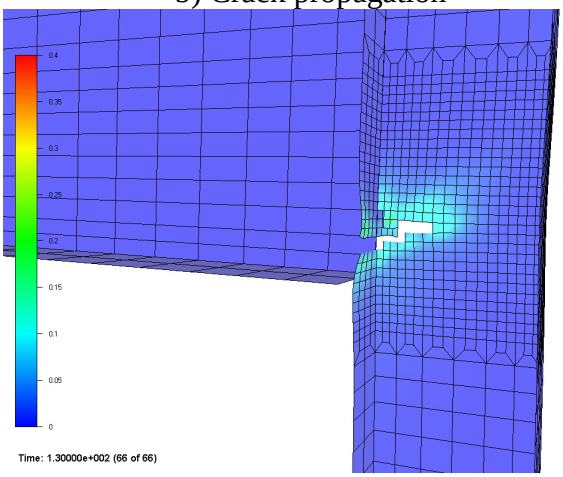

d) Damage and fracture of connection

Figure 3: Numerical result with damaged plasticity model

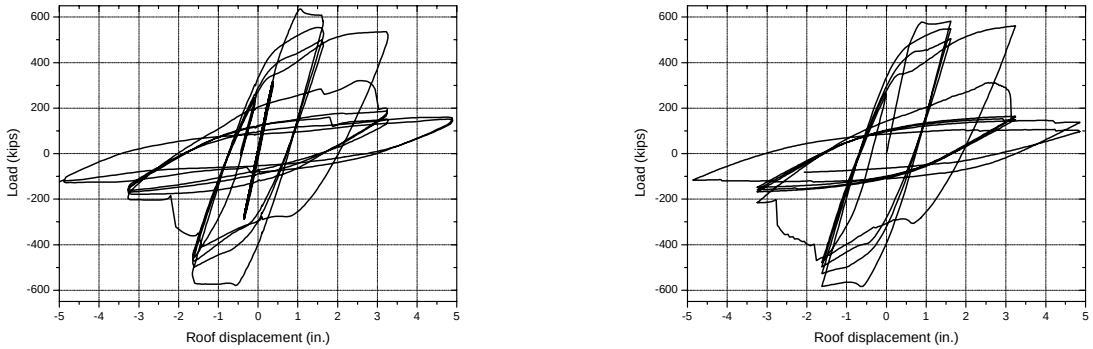

a) Experiment b) Numerical simulation

Figure 4: Load vs. roof displacement for brace frame

Concluding Remarks

The feasibility of a cyclic damaged plasticity model to simulate accurately the behavior of a severely loaded steel braced frame that exhibits local failure of members or connections due to yielding, local buckling and low cycle fatigue has been illustrated. The accuracy of the present finite element analysis depends upon the material constitutive relationships, and in particular, the parameters used. The development of efficient methods for identification of parameters and obtaining more experimental data for calibration are needed.

Acknowledgements

The work preformed in this investigation was funded by the Consortium of Universities for Research in Earthquake Engineering as part of the CUREE-Kajima Joint Research Program on Earthquake Engineering. The authors gratefully acknowledge the funding for this project from the Kajima Corporation, and the leadership of the Joint Oversight Committee in helping define the direction and scope of the research efforts undertaken. In particular, the authors would like to acknowledge the collaboration of Dr. Yoshikazu Sawamoto on this work through sharing of test data, providing advice and a thorough review of the models and results obtained. The assistance of Dr. Patxi Uriz in providing data on braced frames and helping interpret prior test results is gratefully acknowledged.

References

Armstrong, P. J., and Frederick, C. O. (1966). "A Mathematical Representation of the Multiaxial Bauschinger Effect." CEGB Report, RD/B/NN/731, Berkeley Laboratories, R&D Department, CA.

Besson, J., and Guillemer-Neel, C. (2003). "An extension of the Green and Gurson models to kinematic hardening." *Mechanics of Materials*, 35, 1-18.

Cedergren, J., Melin, S., and Lidstrom, P. (2004). "Numerical modeling of P/M steel bars subjected to fatigue loading using an extended Gurson model." *European Journal of Mechanics - A/Solids*, 23, 899-908.

Chaboche, J.-L. (1986). "Time-independent constitutive theories for cyclic plasticity." *International Journal of Plasticity*, 2(2), 149-188.

Chaboche, J.-L. (1989). "Constitutive equations for cyclic plasticity and cyclic visco-plasticity." *International Journal of Plasticity*, 5(3), 247-302.

Coffin, L. F. (1954). "A Study of the Effects of Cyclic Thermal Stresses on a Ductile Metal." *Transations*, ASME, 76, 931-950.

Dufailly, J. and Lemaitre, J. (1995). "Modeling Very Low Cycle Fatigue." *International Journal of Damage Mechanics*, 4, 153-170.

Gurson, A. L. (1977). "Continuum theory of ductile rupture by void nucleation and growth: Part I - yield criteria and flow rules for porous ductile media." *Journal of Engineering Materials and Technology*, ASME, 99, 2-15.

Kachanov, L. M. (1958). "Time of Rupture Process under Creep Conditions." *Ievestiva Akademii Navk SSSR Odtelemie Tekhniheskikh Nauk*, 8, 26-31.

Kanvinde, A., and Deierlein, G. G. (2004). "Micromechanical Simulation of Earthquake Induced Fractures in Steel Structures." *Blume Center Report TR145*, Stanford University, Stanford, CA.

Leblond, J.-B., Perrin, G., and Devaux, J. (1995). "An Improved Gurson-type Model for Hardenable Ductile Metals." *European Journal of Mechanics - A/Solids*, 14, 499-527.

Lemaitre, J. (1992). *A Course on Damage Mechanics*, Springer-Verlag.

Lemaitre, J., and Chaboche, J.-L. (1990). *Mechanics of Solid Materials*, Cambridge University Press.

LSTC (2007). *LS-DYNA® Keyword User's Manual*, Livermore Software Technology Corporation, CA, US.

Manson, S. S. (1953). "Behavior of Materials Under conditions of Thermal Stress." *Heat Transfer Symposium*, University of Michigan Engineering Research Institute, 9-75.

Manson, S. S., Halford, G. R., and Hirschberg, M. H. (1971). "Creep Fatigue Analysis by Strain Range Partitioning." *Symposium on Design for Elevated Temperature Environment*, ASME, NASA, TMX.

Marini, B., Mudry, F., and Pineau, A. (1985). "Ductile Rupture of A508 Steel Under Nonradial loading." *Engineering Fracture Mechanics*, 22(3), 375-386.

McClintock, F. A. (1968). "A Criterion for Ductile Fracture by the Growth of Holes." *Journal of Applied Mechanics*, 35, 363-371.

Morrow, J. D. (1964). "Cyclic Plastic Strain Energy and Fatigue of Metals." *Symposium*, ASTM, Chicago.

Pirondi, A., and Bonora, N. (2003). "Modeling ductile damage under fully reversed cycling." *Computational Materials Science*, 26, 129-141.

Prager, W. (1956). "A New Method of Analyzing Stress and Strains in Work-hardening Plastic Solids." *Journal of Applied Mechanics*, 23, 493-496.

Rice, J. R., Tracey, D. M. (1969). "On the Ductile Enlargement of Voids in Triaxial Stress Fields." *Journal of the Mechanics and Physics of Solids*, 17, 201–217.

Rousselier, G. (1987). "Ductile Fracture Models and Their Potential in Local Approach of Fracture." *Nuclear Engineering and Design*, 105, 97-111.

Steglich, D., Pirondi, A., Bonora, N., and Brocks, W. (2005). "Micromechanical modelling of cyclic plasticity incorporating damage." *International Journal of Solids and Structures*, 42, 337-351.

Tvergaard, V., Needleman, A. (1984). "Analysis of the Cup-cone Fracture in a Round Tensile Bar." *Acta Metallurgica*, 32(1), 157-169.

Tvernelli, J. F., and Coffin, L. F. (1959). "A Compilation and Interpretation of cyclic Strain Fatigue Tests on Metals." *Transations*, ASM, 51, 438-453.

Uriz, P., and Mahin, S. (2004). "Seismic Performance Assessment of Concentrically Braced Steel Frames." *Proceedings of the 13th World Conference on Earthquake Engineering*.

Xia, L., and Shih, C. F. (1995). "Ductile Crack Growth-I. A Numerical Study Using Computational Cells with Microstructurally-based Length Scales." *Journal of the Mechanics and Physics of Solids*, 43(2), 233-259.

Ziegler, H. (1959). "A Modification of Prager's Hardening rule." *Quarterly of Applied Mechanics*, 17, 55-65.